Experimental observation of four-wave resonant interaction: from low steepness to wave breaking

F. Bonnefoy[1*], F. Haudin[2], G. Michel[3], B. Semin[3], T. Humbert[4], S. Aumaître[4], M. Berhanu[2], and E. Falcon[2]

1 – LHEEA, Centrale Nantes, Nantes, France
2 – MSC, Université Paris Diderot, CNRS, Paris, France
3 – LPS, Ecole Normale Supérieure, CNRS, Paris, France
4 – SPEC, Univ. Paris-Scalay, CEA-Saclay, CNRS, Gif-sur-Yvette, France
[*] felicien.bonnefoy@ec-nantes.fr

HIGHLIGHT
We experimentally study resonant interactions of oblique surface gravity waves in a large basin. We generate two oblique waves crossing at an acute angle, while we control their frequency ratio, steepnesses and directions. These mother waves mutually interact and give birth to a resonant daughter wave whose properties (growth rate, resonant response curve and phase locking) have been fully characterized in Bonnefoy et al. (2016) at low steepness. Our results strongly extend previous experimental results performed mainly for perpendicular or collinear wave trains. Waves with stronger steepness produce new daughter waves that are measured and explained by means of Zakharov theory. Resulting oblique wave packets are observed which are explained as the interference between these daughter waves generated in a cascade by the four-wave interactions.

1 INTRODUCTION

Nonlinear resonant interactions among three waves and and four waves are efficient mechanisms to transfer energy between scales. Four-wave interactions studies for water waves started in the early theoretical works of Phillips (1960) and Longuet-Higgins (1962). Four-wave interactions occur if interacting waves fulfil the two resonance conditions $\boldsymbol{k}_1 + \boldsymbol{k}_2 = \boldsymbol{k}_3 + \boldsymbol{k}_4$ and $\omega_1 + \omega_2 = \omega_3 + \omega_4$, where the angular frequencies ω_i and wavevectors $\boldsymbol{k}_i$ are linked by the dispersion relation $\omega_i = \omega(\boldsymbol{k}_i)$. Mainly for the sake of simplicity, special attention has been given to the case of two degenerated waves, i.e. $\boldsymbol{k}_1 = \boldsymbol{k}_2$. Surprisingly, there exist only few experiments specifically devoted to studying such resonant wave interactions between water waves. Longuet-Higgins & Smith (1966) and McGoldrick et al. (1966) were the first to observe the generation of a daughter wave $\boldsymbol{k}_4$ by wave interactions in the degenerated case with perpendicular mother waves $\boldsymbol{k}_1 \perp \boldsymbol{k}_3$. These pioneering works were restricted to perpendicular mother waves with fixed and strong wave steepness ($\varepsilon = ka$ =0.1, with a the wave amplitude) within a relatively small basin (3 m). In the same perpendicular configuration, Tomita (1989) confirmed the daughter growth rate to greater distances within a larger basin (54 m), still for fixed, but lower, mother-wave steepness ($\varepsilon < 0.05$).
We have extended recently this experimental validation of Longuet-Higgins theory to oblique waves crossing with an acute angle, as shown in Bonnefoy et al. (2016). At low steepness (ε =0.05), all our results are in good quantitative agreement with four-wave interaction theory with no fitting parameter. The experiments presented in Bonnefoy et al. (2016) correspond to the early stage of resonance, when the nonlinear distance $k_4 \varepsilon^2 d < 1$ where d is the distance from the wavemaker.
We present here our experimental observations with increasing steepness, at greater distance $k_4 \varepsilon^2 d$. We choose hereafter to generate the degenerated resonant mother waves which are those with the maximum growth rate of the daughter wave in order to get significant measurements.

2 EXPERIMENTAL SETUP

The experiments presented here were designed to test the resonance theory for wave directions different from the perpendicular case studied in the 1960s and by Tomita (1989) (see Bonnefoy et al. (2016)). We mechanically generate bichromatic waves (mother waves 1 and 3 with frequencies ω_1 and ω_3) in a rectangular wave basin and observe the birth of the daughter wave of frequency $2\omega_1 - \omega_3$ due to resonant interaction. The wave basin at Ecole Centrale de Nantes has dimensions 50 m-30 m-5 m and its wavemaker consists of 48 independent flaps that are hinged 2.8 m below the free surface. Fig. 1 (left) shows a top view of the set-up. In order to avoid spurious reflections on the sidewalls, the motion of the segmented wavemaker is controlled by means of the method of Dalrymple (1989). The Dalrymple method aims at generating the target wave field at a distance X_d =10 m from the wavemaker and yields a quasi-uniform wave field from the wavemaker up to 25 m (see the grey zone of Fig. 1 (left)); this is crucial for these interaction experiments.

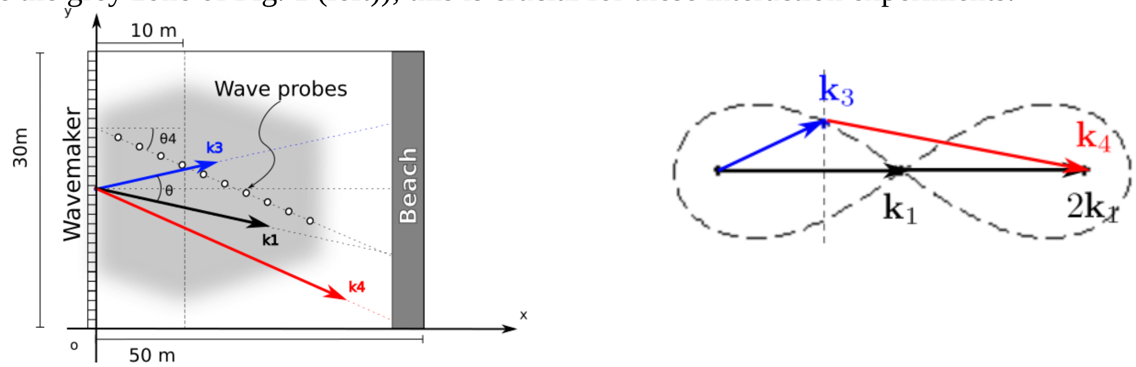

Fig. 1 Left: wave basin showing the homogeneous zone (shaded area), the wave probes (circles) and the wavevectors $\boldsymbol{k}_1$, $\boldsymbol{k}_3$ and $\boldsymbol{k}_4$ for the maximum growth rate case (arrows respectively in green, red and blue). Right: Figure of eight from Phillips (1960) with the degenerated resonant quartet corresponding to the maximum growth rate of the daughter wave.

The input parameters to the wavemaker are mother-wave frequency (f_1 and f_3), steepness (or amplitude a_1 and a_3) and direction (θ_1 and θ_3 with respect to the basin main axis). The daughter-wave direction is defined as θ_4 in the wave basin. In Bonnefoy et al. (2016), frequencies for the mother waves are chosen to fit the basin capacities: fixed f_1 =0.9 Hz (wavelength λ_1 =2 m) and varied $f_3 = f_1/r$ with r =0.8–1.6. The corresponding wavelengths λ_3 ranged from 1.3 to 4 m. The angle $\theta_3 - \theta_1$ between mother waves 1 and 3 was varied between -15° and 40°.

In the present case, we generate the resonant mother waves corresponding to the maximum growth rate of the daughter wave, which have the parameters f_1 =0.9 Hz, f_3 =0.714 Hz ($r = r_m = 1.258$) and $\theta = \theta_m$ =25°. During our tests, we made the mother wave directions in the basin being symmetrical, that is $\theta_3 = -\theta_1 = \theta_m/2$, in order to minimize sidewall effects. The resulting direction of the daughter wave is $\theta_4 = \theta_{4m} = -23.1°$.

A linear frame supporting an array of twelve resistive wave probes is set up in this direction θ_{4m} (see Fig. 1, left). The distance between two successive probes is approximately 2 m. The distance d to the wavemaker and measured along the direction of the daughter wave ranges from d =2.5 to 25 m. The sampling frequency is 100 Hz and wave elevation signals were recorded during approximately 100 s, which corresponds to a steady regime of more than 50 wave periods. Typical amplitudes are $a_{1,3}$= few cm for mother waves and a_4 from a few mm to 1 cm for daughter waves.

3 EXPERIMENTAL OBSERVATION FOR HIGH STEEPNESS

We generate the resonant oblique waves $\boldsymbol{k}_1$ and $\boldsymbol{k}_3$ in degenerated interaction as defined above. Fig. 2 shows a picture of the resulting wavefield in steady state. These mother waves interact and give birth to the daughter wave $\boldsymbol{k}_4$. This daughter wave can be observed on Fig. 3, left which plots the magnitude of the Fourier transform of the elevation recorded at large distance from the wavemaker. Next to the main peaks at frequency f_1 and f_3, one can see one first secondary peak at frequency $f_4 = 2f_1 - f$_3. For a low steepness, these peaks are the only one we see around the main peaks (Bonnefoy et al. (2016)). Here however we also find other wave components with frequencies are defined by $f_{n+2} = nf_1 - (n-1)f_3$.

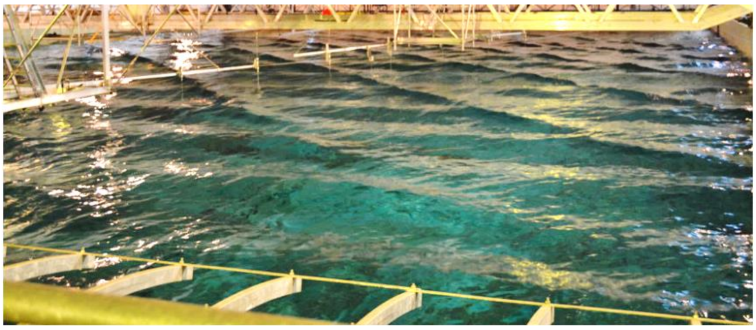

Fig. 2 View of the wave field in steady regime (after wave fronts) in resonant conditions with $\boldsymbol{r = r_m}$ and $\boldsymbol{\varepsilon_1 = \varepsilon_3 = 0.14}$

They are formed by new four wave interactions involving the mother waves and the daughter waves when the latter have significant amplitudes to create new daughter waves through quasi-resonant 4-waves interactions, either in a degenerated situation or not. Fig. 3, right shows the corresponding wave-numbers. For instance, we may define two quartets producing child wave $\boldsymbol{k}_5$ by $\boldsymbol{k}_5 = \boldsymbol{k}_1 + \boldsymbol{k}_4 - \boldsymbol{k}_3$ or $\boldsymbol{k}_5 = 2\boldsymbol{k}_4 - \boldsymbol{k}_1$. The first interaction is near resonance ($\omega_5 \cong \omega_1 + \omega_4 - \omega_3$) while the second shows a significant detuning ($\omega_5 + \omega_1 - 2\omega_4 \neq 0$).

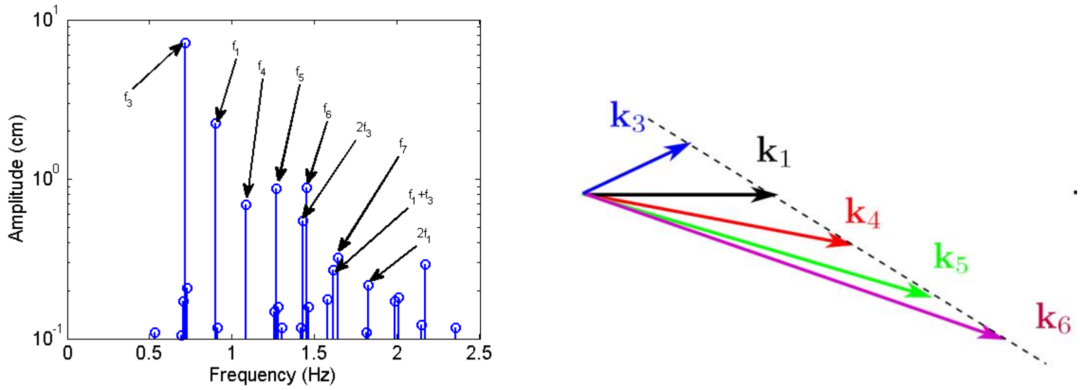

Fig. 3 Left: frequency spectrum of wave elevation recorded at d =21.5 m. The vertical axis is plotted with log scale. Wave conditions $\boldsymbol{r = r_m}$, $\boldsymbol{\theta = \theta_m}$ and $\boldsymbol{\varepsilon_1 = \varepsilon_3 = 0.14}$. Right: wavenumbers involved in the cascade of quasi-resonant interactions.

4 THEORETICAL APPROACH

The spatial evolution of the new waves is compared to the numerical solution of the Zakharov equation which may be written

$$i\partial_t B_1 = \int T_{1234} B_2^* \, B_3 \, B_4 \, \delta_{1+2-3-4} \exp(\Delta_{1234} t) \, d\boldsymbol{k}_2 d\boldsymbol{k}_3 d\boldsymbol{k}_4$$

where $B_i = B(\boldsymbol{k}_i, t)$ is the wave action, $\Delta_{1234} = \omega_1 + \omega_2 - \omega_3 - \omega_4$ is the linear detuning. The interaction coefficients $T_{1234} = T(\boldsymbol{k}_1, \boldsymbol{k}_2, \boldsymbol{k}_3, \boldsymbol{k}_4)$ are the kernels given in Krasitskii (1994) or Janssen (2009). We have also $\delta_{1+2-3-4} = \delta(\boldsymbol{k}_1 + \boldsymbol{k}_2 - \boldsymbol{k}_3 - \boldsymbol{k}_4)$. If the wavefield is described by the superposition of the two mother waves $\boldsymbol{k_1}$ and $\boldsymbol{k_3}$ plus the daughter wave $\boldsymbol{k_4}$ (the wave action is taken as $B(\boldsymbol{k}, t) = B_1(t)\delta(\boldsymbol{k} - \boldsymbol{k_1}) + B_3(t)\delta(\boldsymbol{k} - \boldsymbol{k_3}) + B_4(t)\delta(\boldsymbol{k} - \boldsymbol{k_4})$), then the Zakharov equation provides the temporal evolution equation for the mother waves (e.g. mother wave 1 energy is pumped into wave 3 and 4, not shown here), the daughter waves 4 and also for two extra short waves 5 and 6 which are usually neglected at low steepness. Wave 5 for instance satisfies $i\partial_t B_5 = 2T_{1435} \exp(\Delta_{1435} t) + T_{4415} \exp(\Delta_{4415} t)$. Adding wave 5 in the wave action B refines the evolution equation for all existing wave components and provides approximate equations for new waves 6 to 8. Fig. 4 shows the evolution of the waves $\boldsymbol{k_4}$ to $\boldsymbol{k_7}$ along the basin for experiments where the steepness, equal for both mother waves $\varepsilon = \varepsilon_1 = \varepsilon_3$, is increasing. Note that the time domain solution of the Zakharov equation is converted into space dependence in the basin by means of the group velocity of the slowest wave. The measured daughter waves steepness is normalized with ε as a function of the nonlinear distance $k_4 d\varepsilon^2$.

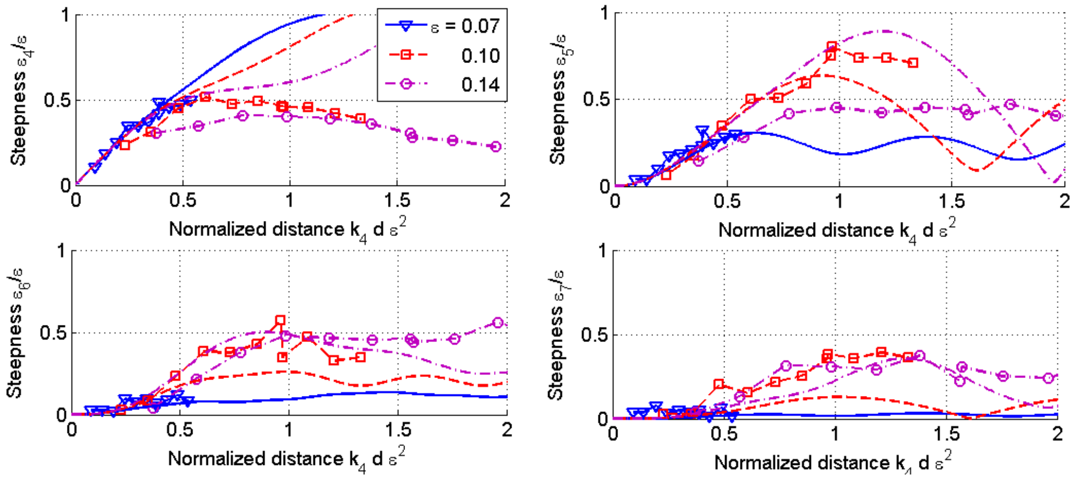

Fig. 4 Normalized steepness evolution with nonlinear distance. The lines with markers are the experimental results for 3 increasing mother waves steepness ($\varepsilon = \varepsilon_1 = \varepsilon_3$). The lines without marker correspond to the numerical solution of the Zakharov equation written with initial waves k_1, k_3, k_4 and k_5.

The results shown in Fig. 4 present a good agreement between Zakharov theory and experiments for waves 4, 5 and 6 which means that the dominant transfer is well captured by the chosen model with 4 initial waves 1, 3, 4 and 5. Note that waves 4 to 6 have similar steepness around $\varepsilon/2$ for strong steepness $\varepsilon = 0.14$ and that accurately predicting wave 7 evolution would require more terms in the Zakharov model.

During experiments were also noticed oblique wave packets, visible for instance in the upper part of Fig. 2. Those packets were accompanied with localized breakers. The superposition of the two mother waves plus the daughter waves is a good candidate to explain the origin of these groups. As an illustration of the possible interference patterns, Fig. 5, top shows the superposition of waves 1 and 3 oriented as in the wave basin experiments; nodes and antinodes are oriented perpendicular to $\boldsymbol{k}_1 - \boldsymbol{k}_3$. Fig. 5, bottom plot superimposes this bichromatic wave plus waves $\boldsymbol{k}_4$, $\boldsymbol{k}_5$ and $\boldsymbol{k}_6$. The group pattern is formed, with thin nodes and short waves with high amplitudes and large antinodes. The breakers are then prone to appear near these steep nodes, as observed in the basin.

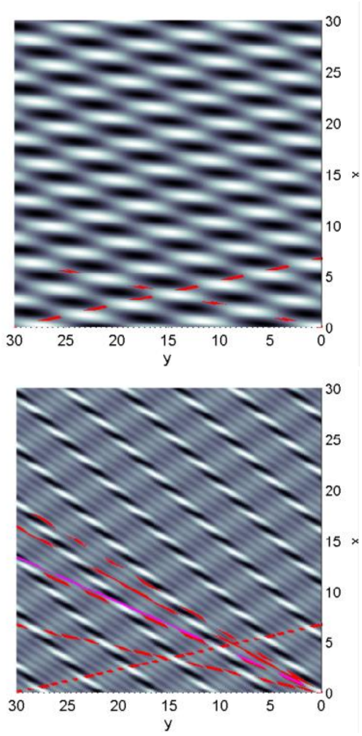

Fig. 5 Superposition of sine waves
Top: $A(x) = \cos \boldsymbol{k}_1.\boldsymbol{x} + \cos \boldsymbol{k}_3.\boldsymbol{x}$
Bottom: $B(x) = A(x) + \cos \boldsymbol{k}_4.\boldsymbol{x} + \cos \boldsymbol{k}_5.\boldsymbol{x} + \cos \boldsymbol{k}_6.\boldsymbol{x}$

REFERENCES

Bonnefoy, F. et al., 2016. J. Fluid Mech., 805 R3, 1-12.
Dalrymple, R.A., 1989. J. Hydraulic Research, 27(1), 23–34.
Janssen, P. A. E. M., 2009. J. Fluid Mech., 637, 1–44.
Krasitskii, V. P., 1994. J. Fluid Mech., 272, 1 – 20.
Longuet-Higgins, M. S., 1962. J. Fluid Mech., 12, 321–32.
Longuet-Higgins, M. S. and Smith, N. D., 1966. J. Fluid Mech., 25, 417–435.
McGoldrick, L. F. et al., 1966. J. Fluid Mech., 25, 437–456.
Phillips, O. M., 1960. J. Fluid Mech., 9, 193–217.
Tomita, H., 1989. Report of Ship Res. Inst., NMRI, 26(5), 251–350.
Zakharov, V., 1968. J. Appl. Mech. Tech. Phys., 2, 190–198.